






Article

# Effect of Mesoporous Silica Nanoparticles on Glycerol-Plasticized Anionic and Cationic Polysaccharide Edible Films

Concetta Valeria Lucia Giosafatto <sup>1,\*</sup>, Mohammed Sabbah <sup>1,2</sup>, Asmaa Al-Asmar <sup>1,3</sup>,  
Marilena Esposito <sup>1</sup>, Alfredo Sanchez <sup>4</sup>, Reynaldo Villalonga Santana <sup>4</sup>, Marcella Cammarota <sup>5</sup>,  
Loredana Mariniello <sup>1</sup>, Prospero Di Piero <sup>1</sup> and Raffaele Porta <sup>1</sup>

<sup>1</sup> Department of Chemical Sciences, University of Naples “Federico II”, 80126 Naples, Italy; marilena.esposito2@unina.it (M.E.); loredana.mariniello@unina.it (L.M.); dipierro@unina.it (P.D.P.); raffaele.porta@unina.it (R.P.)

<sup>2</sup> Department of Nutrition and Food Technology, An-Najah National University, P.O. Box: 7 Nablus, Palestine; m.sabbah@najah.edu

<sup>3</sup> Analysis, Poison control and Calibration Center (APCC), An-Najah National University, P.O. Box 7 Nablus, Palestine; asmaa.alasmar@unina.it

<sup>4</sup> Department of Analytical Chemistry, Faculty of Chemistry, Complutense University of Madrid, 28040 Madrid, Spain; alfredos@ucm.es (A.S.); rvillalonga@quim.ucm.es (R.V.S.)

<sup>5</sup> Department of Experimental Medicine, University of Campania “Luigi Vanvitelli”, 80138 Naples, Italy; marcella.cammarota@unicampania.it

\* Correspondence: giosafat@unina.it; Tel.: +39-081-253-9470

Received: 5 February 2019; Accepted: 2 March 2019; Published: 5 March 2019



**Abstract:** This study describes the production of reinforced polysaccharide (PS)-based films, by adding mesoporous silica nanoparticles (MSNs), to either pectin (PEC) or chitosan (CH) film forming solutions, either containing glycerol (GLY) as a plasticizer, or not. Film characterization demonstrated that MSNs and GLY were able to significantly increase the plasticity of both PS-based biomaterials and that the interactions between PSs and nanoparticles were mainly due to hydrogen bonds. Moreover, MSN-containing films were less transparent, compared to controls prepared with either PEC or CH, in the absence of GLY, while all films containing MSNs, but obtained with the plasticizer, were as transparent as the films prepared with PEC or CH alone. MSN addition did not influence the thickness of the PEC-based films, but increased that of CH-based ones, prepared both in the absence and presence of GLY. MSN-containing PEC-based films possessed a more compact and homogeneous morphology, with respect to both control films, prepared, with or without GLY, and to the CH-based films, containing MSNs, the structure of which showed numerous agglomerations. Finally, moisture content and uptake were reduced, in all films prepared in the presence of MSNs. The suggested addition of MSNs might have given rise to novel biomaterials for food or pharmaceutical applications.

**Keywords:** chitosan; pectin; silica nanoparticles; edible films; glycerol

## 1. Introduction

In the last decades, there has been a worldwide demand for replacing the highly pollutant oil-based plastics, by renewable and biodegradable materials. In fact, there has been an increased interest in the development and application of biodegradable/edible films and coatings in the food industry, as a consequence of the increasing consumer demand for safe and stable functional foods, with a low environmental impact [1]. Ideal candidates for reducing the huge amount of conventional plastics are the “bioplastics, manufactured exclusively with natural polymers, which are able to be fully

recycled into the environment, in a short time, following their utilization as packaging materials” [2–4]. Renewable resources for producing bioplastics are represented by several polysaccharides (PSs) that are able to constitute the matrices for edible films and coatings [5,6]. Nevertheless, films based on natural polymers are widely known to exhibit poor mechanical resistance, as well as limited barrier and thermal properties. Consequently, these biomaterials had so far restricted commercial applicability in the food packaging sector. More recently, much attention has been given to the production of biopolymer composites, where at least one of their components has nanometric dimensions (1–100 nm) [7]. Such nanoreinforcement is due to the nanoparticles of different chemical natures that are added to a variety of biopolymers, with the aim of obtaining biomaterials with enhanced mechanical and other chemico-physical properties. A uniform nanoparticles dispersion, within a polymer matrix, leads to a very large matrix/filler interfacial area, which changes the molecular mobility, the relaxation behavior, and the resulting thermal, and tensile properties of the material. In this context, special consideration was given to the mesoporous silica nanoparticles (MSNs), due to their unique features, such as the high surface area, controllable pore structure, large pore volume, optically transparent properties, low toxicity, high chemical and thermal stability, and versatile chemically modifiable surface [8]. These nanoparticles act as material reinforcements because they allow an intercalation/exfoliation of silicate layers in the polymer matrix, and therefore, their use is turning into a promising option, to improve the technological features of biopolymer-based films. Hence, the objective of the present work was the reinforcement of either pectin (PEC) or chitosan (CH)-based films, by means of MSNs. PEC is an anionic PS, occurring in fruits and numerous vegetables which represents the major structural component of cell walls [9]. It is currently used in fruit jellies, pharmaceuticals, and cosmetics, for its thickening and emulsifying properties, and ability to solidify to a gel [10]. Conversely, CH is a cationic biopolymer being derived from the deacetylation of chitin [11], the second most abundant polysaccharide, existing in nature, mainly found in the exoskeleton of crustaceans, and in fungal cell walls. CH is frequently used in designing drug delivery systems, because of its biodegradability, non-toxicity, antibacterial, and hemostatic characteristics. Despite the individual advantages, both PSs give rise to films, with some drawbacks, due to their brittleness and poor mechanical and moisture barrier properties. Hence, PEC-MSN and CH-MSN biocomposites, plasticized with glycerol (GLY) or not, have been prepared and partially characterized to find possible applications of the novel biomaterials, both in food and pharmaceutical sectors.

## 2. Materials and Methods

### 2.1. Materials

Citrus peel low-methylated (7%) PEC (Aglupectin USP) was purchased from Silva Extracts s.r.l. (Gorle, BG, Italy). CH (mean molar mass of  $3.7 \times 10^4$  g/mol) with a degree of 9.0% N-acetylation, was purchased from Professor R.A.A. Muzzarelli (University of Ancona, Italy) [12]. GLY was obtained from the Merck Chemical Company (Darmstadt, Germany). MSNs were prepared and characterized, as recently reported by Fernandez-Bats et al. [8]. All other chemicals and solvents were of analytical grade.

### 2.2. Film Preparation

PEC-based film forming solutions (0.6% w/v) were prepared from a PEC stock solution (2% w/v of water), at pH 7.5. CH-based film forming solutions (0.6% w/v) were prepared from a CH stock solution (2% w/v of hydrochloric acid 0.1 N, stirred overnight) at a pH 4.5. All film forming solutions, with added MSNs or not (3% w/w of PEC or CH), were prepared in the absence or presence of GLY (30% w/w of PEC or CH), in 50 mL of distilled water and characterized, as previously described [12,13]. The film forming solutions were then cast onto 8 cm diameter polycarbonate Petri dishes and allowed to dry in an environmental chamber, at 25 °C and 45% Relative Humidity (RH) for 48 h. The dried films were peeled, intact, from the casting surface and tested, as described below.

### 2.3. Film Thickness and Opacity

The thickness was performed for each film, in six different points, with a digital micrometer (DC-516, sensitivity 0.001 mm). The opacity test measurements, carried out six times for each sample, were performed, as described by Tonyali et al. [14]. Opacity was calculated as follows:

$$\text{Opacity (mm}^{-1}\text{)} = A_{600}/x \quad (1)$$

where  $A_{600}$  was the absorbance at 600 nm and  $x$  was the film thickness (mm).

### 2.4. Film Mechanical Properties

Mechanical properties of films, namely tensile strength, elongation at break, and Young's modulus, were obtained by using a universal testing instrument Model No. 5543A (Instron, Norwood, MA, USA). The obtained films were cut into strips (10 mm  $\times$  50 mm), by using a sharp razor blade. Each strip was conditioned in an environmental chamber, at 25 °C and 50% RH, for 2 h. Finally, six strips of each film type were tested. The mechanical properties were measured, according to the ASTM D882-97 [15].

### 2.5. Morphology Analysis (SEM)

Film surfaces and cross-sections were analyzed by Scanning Electron Microscope (SEM). Films were cut using scissors, mounted onto a stub, and sputter-coated with platinum–palladium (Denton Vacuum Desk V), before being observed by the Supra 40 ZEISS (EHT = 5.00 kV, in lens detector). Micrographs for sample surfaces were obtained at 25,000 $\times$  magnifications, whereas cross-sections were obtained at both 25,000 $\times$  and 50,000 $\times$  magnifications.

### 2.6. Fourier Transform Infrared (FT-IR) Spectra

FT-IR measurements of the films were performed by a Bruker model ALPHA spectrometer (Bruker model ALPHA spectrometer, Leipzig 04318, Germany) equipped with attenuated total reflectance (ATR) accessory. The measurements were obtained in 4,000–400  $\text{cm}^{-1}$  region, at 4  $\text{cm}^{-1}$  resolution for 24 scans.

### 2.7. Film Moisture Content

Moisture content of each film was measured gravimetrically, according to Farhan and Hani [16], and Singh et al. [17], with some modifications. In particular, test specimens (5 cm  $\times$  5 cm) at different positions of each film type were uniformly cut and placed on glass Petri dishes. Film moisture content was determined by drying each specimen in an oven, at 105 °C, until a constant dry weight was obtained. Film moisture content was calculated as:

$$\text{Film moisture content (\%)} = (W_1 - W_2)/W_1 \times 100, \quad (2)$$

where  $W_1$  is the initial weight of the film and  $W_2$  is the film weight, after drying at 105 °C, overnight. Each measure was carried out in triplicates.

### 2.8. Film Moisture Uptake

Moisture uptake of each film was measured, gravimetrically, in triplicates, as described by Manrich et al. [18]. In particular, films were cut into 5-cm-sided squares, dried at 105 °C for 24 h, conditioned at  $23 \pm 2$  °C, into a desiccator, previously equilibrated at 50% RH, with a saturated  $\text{Mg}(\text{NO}_3)_2$  solution for 24 h. The moisture uptake was calculated as:

$$\text{Film moisture uptake (\% dry matter)} = (W_s - W_d)/W_s \times 100, \quad (3)$$

where  $W_s$  and  $W_d$  are the weight of the swollen (24 h at 50% RH) and the dried films, respectively. Each measure was carried out in triplicates.

### 2.9. Statistical Analysis

All data were analyzed by the JMP software (SAS Institute, Cary, NC, USA, version 5.0). The data were subjected to analysis of variance, and the means were compared, using the Tukey–Kramer HSD "honestly significant difference" test. Differences were considered to be significant at  $p < 0.05$ .

## 3. Results and Discussion

### 3.1. Film Thickness and Opacity

Thickness is a useful parameter, as it serves as a basis for determining several functional properties of the films. As for CH-based films, the data reported in Table 1 indicates that the thickness value significantly increased when MSNs were presented into the film matrix, whereas the addition of MSNs did not lead to a statistically significant change of PEC-based film thickness. This result could be explained with the increase of viscosity of nanoparticle-containing CH-based film-forming solution [7], which is able to affect the spreadability and thickness of the derived materials [19]. Conversely, the addition of GLY to the film-forming solutions was observed to increase the thickness of the CH-based, as well as of that of the PEC-based films. In addition, in the presence of both GLY and MSNs, CH film thickness resulted in almost three-times greater than that measured with films made by CH alone. Since the appearance of the coated foods plays an important role in consumer acceptability, the opacity of the biomaterials was evaluated, by measuring the light transmission through the films, at a wavelength of 600 nm. Table 1 clearly indicates that the opacity values of both PEC- and CH-based films, markedly increased, when MSNs were present into the film matrices and GLY was absent. Nevertheless, it is worthy to note that the concomitant presence of GLY had a remarkable effect in decreasing film opacity, since the MSNs-containing both CH- and the PEC-based films appeared to be transparent, as the control films, thus, indicating that the GLY allowed to obtain a more homogenous nanoparticle dispersion inside the film matrix, as it was confirmed by SEM experiments (see below).

### 3.2. Film Mechanical Properties

We have previously observed that the mechanical properties of protein-based films were significantly improved in the presence of MSNs, reaching the maximum values, at a concentration of 3% of nanoparticles [8]. In addition, 30% GLY concentration was found to satisfactorily plasticize the PS-based films [12,13]. Therefore, we selected such a formulation of film-forming solutions to compare the tensile strength, elongation at break, and the Young's modulus of the nanoparticle-containing films, to those of the control films. Table 1 shows that both MSN and GLY were able to significantly increase the plasticity of, both, the PEC- and the CH-based biomaterials. As for the PEC-based films, MSN, and GLY alone, increased the film elongation at break, and reduced Young's modulus, even though a more marked effect on these parameters was obtained by adding both MSN and GLY. At the same time, the concurrent presence of nanoparticles and plasticizer significantly reduced the tensile strength of the PEC-based films. Similar results were obtained by analyzing the CH-based biomaterial, even though, in this case, GLY alone exhibited the most plasticizing effect. Conversely, previously reported data on the MSN effects on the mechanical properties of protein-based films, showed a concomitant increase of both tensile strength and elongation at break [8], thus, indicating different interactions of the same nanoparticles grafted into the matrices of different biopolymer nature.

**Table 1.** Effect of mesoporous silica nanoparticles (MSNs) on film thickness, transparency, and mechanical properties of the pectin (PEC) and the chitosan (CH) films plasticized with glycerol (GLY), or not.

Film	Thickness ( $\mu\text{m}$ )	Opacity ( $\text{mm}^{-1}$ )	Tensile Strength (MPa)	Elongation at Break (%)	Young's Modulus (MPa)
<b>PEC-based</b>					
Control	37.5 $\pm$ 1.3	1.91 $\pm$ 0.16	33.4 $\pm$ 7.8	0.8 $\pm$ 0.2	5750.2 $\pm$ 612.2
+ MSN	40.1 $\pm$ 1.2	3.63 $\pm$ 0.72 *	40.8 $\pm$ 2.5	2.2 $\pm$ 0.7	3732.5 $\pm$ 264.0 *
+ GLY	56.8 $\pm$ 2.5 *	2.05 $\pm$ 0.28	27.7 $\pm$ 4.4	9.4 $\pm$ 2.5 *	1067.6 $\pm$ 49.3 *
+ MSN + GLY	58.2 $\pm$ 2.1 *	1.88 $\pm$ 0.29	16.6 $\pm$ 2.4 *	15.2 $\pm$ 1.4 *	712.3 $\pm$ 52.4 *
<b>CH-based</b>					
Control	30.1 $\pm$ 3.1	2.20 $\pm$ 0.28	56.2 $\pm$ 4.2	7.7 $\pm$ 1.8	3438.1 $\pm$ 501.3
+ MSN	51.3 $\pm$ 1.2 *	6.62 $\pm$ 1.88 *	42.4 $\pm$ 8.3	13.0 $\pm$ 5.6	2088.8 $\pm$ 137.3 *
+ GLY	61.2 $\pm$ 2.3 *	1.44 $\pm$ 0.89	12.5 $\pm$ 2.3 *	82.5 $\pm$ 2.0 *	130.5 $\pm$ 52.2 *
+ MSN + GLY	81.7 $\pm$ 3.7 *	1.87 $\pm$ 0.35	28.1 $\pm$ 2.2 *	54.9 $\pm$ 4.2 *	427.3 $\pm$ 64.2 *

\* Values significantly different at  $p < 0.05$  from those obtained without MSN and GLY.

### 3.3. Film Morphology

Figure 1 shows the images of the different films and their surfaces and cross-sections obtained from the SEM analysis. The control, PEC-based films, prepared in the absence of GLY and MSNs, appeared to be more compact and homogenous, in both, the surface (Figure 1, A1) and the cross-section (Figure 1, inset A2), than the control CH films (Figure 1, insets C1 and C2). The presence of MSNs conferred to the surface of the PEC-based films, prepared either in the presence or absence of GLY, an even more compact and homogeneous structure, compared to the control films, probably due to a widespread inclusion of MSNs, into the PEC network responsible for the major smoothness of the matrices obtained (Figure 1, inset A3 and B3). This hypothesis seemed to be confirmed from the film cross-section SEM images, at 25,000 $\times$  magnification, which shows a more compact and homogeneous structure of the MSN-containing film matrices, exhibiting more evident continuous zones, in comparison with the control sample (Figure 1, inset A4 and B4), as well as from the zoomed SEM micrographs (obtained at 50,000 $\times$  magnification), showing the pervasive inclusion of nanoparticles in the PEC film matrix (Figure 1, inset A5 and B5). Numerous aggregations were observed, by contrast, in the cross-sections of the CH-based films prepared in the presence of MSNs, without (Figure 1, inset C4 and C5) or with (Figure 1, inset D4 and D5) GLYs. In fact, these films exhibited many protuberances or fractured morphology, probably due to the MSNs interactions with the CH chains. These results were similar to those reported by Liu et al. [20], who found that the ultrastructure of the starch-based materials was much rougher and exhibited numerous aggregations, due to the asymmetrical MSN dispersion in the film matrix.

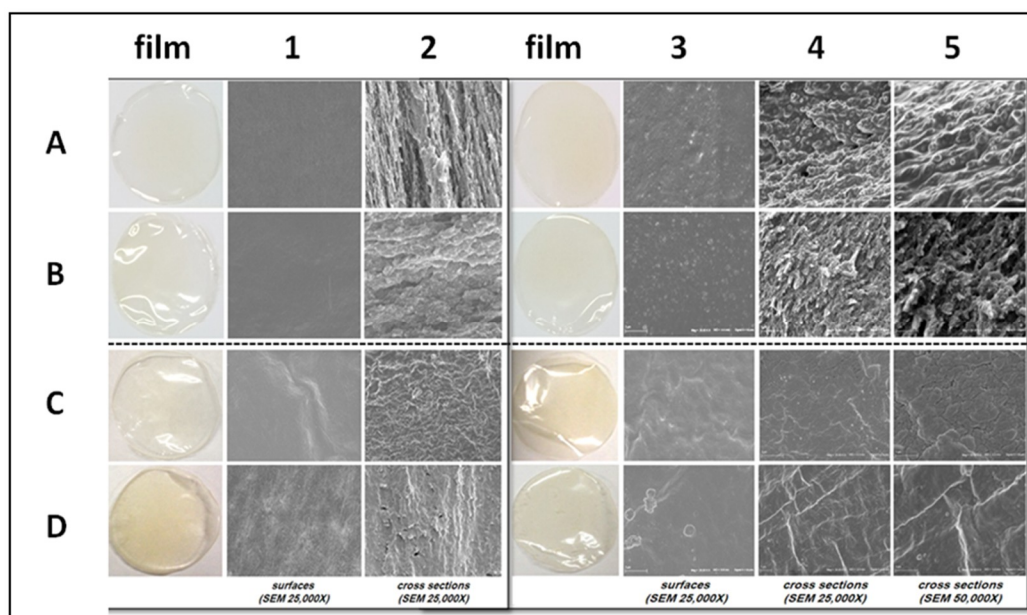


**Figure 1.** SEM morphology of the PEC (A,B) and the CH (C,D) films, prepared in the absence (A1,A2,C1,C2) or presence of either GLY (B1,B2,D1,D2), MSN (A3–5,C3–5), or both GLY and MSN (B3–5,D3–5).

#### 3.4. Film FT-IR Analyses

To elucidate the molecular interactions of both PEC and CH with MSNs, all films were also analyzed by the ATR-FT-IR (Figure 2). The bands detected in the region below  $1,000\text{ cm}^{-1}$  arose from inter-atomic vibrations, the bands around  $832$  and  $400\text{ cm}^{-1}$ , being characteristic of the silanol groups (Si–OH), and being related to the Si–O stretching and deformation frequencies [21,22]. The spectra of all PEC-based films (Figure 2, panel A) results were quite similar, representing bands originating from the vibrations of the functional groups of the compounds existing in their matrices, and showing only some differences in the relative intensities and positions. Nesic et al. [23] reported that the interactions between the PEC and the silica, occur between the hydroxyl groups of the PS and the oxygen containing groups of MSNs. The absorption bands in the range between  $3,400$  and  $3,000\text{ cm}^{-1}$  and  $1,410\text{ cm}^{-1}$  were typical of hydroxyl groups of bound water, as well as of Si–OH linkage [24], whereas the peaks at  $1,751$  and  $1,628\text{ cm}^{-1}$ , corresponded to the C=O stretching of esterified carboxylic groups (–COOCH<sub>3</sub>) and free carboxylic groups (–COOH), respectively. The stretching, asymmetric, symmetric, and deformation vibrations of the siloxane network, could be identified with the bands around  $1,177\text{ cm}^{-1}$  [25]. All these interactions were more marked in the CH film (Figure 2, panel B) spectra, showing a broad band at  $3,267\text{ cm}^{-1}$ , apparently related to the hydroxyl and amino groups occurring on the polysaccharide chains [26]. Finally, the band at  $2,881\text{ cm}^{-1}$  was assigned to the C–H stretching vibrations, the band near  $1,461\text{ cm}^{-1}$  owed to the stretching frequency of the carbonyl amidic groups present within the CH chains, with some degree of acetylation, whereas the band in the range of  $1,250$ – $1,030\text{ cm}^{-1}$  was related to the asymmetric stretching vibration of the Si–O–Si group. In conclusion, all the film FT-IR data showed evident interactions of the PS matrix, with both GLY and MSNs, by hydrogen bonds, and these interactions became increasingly pronounced in the CH-based films.

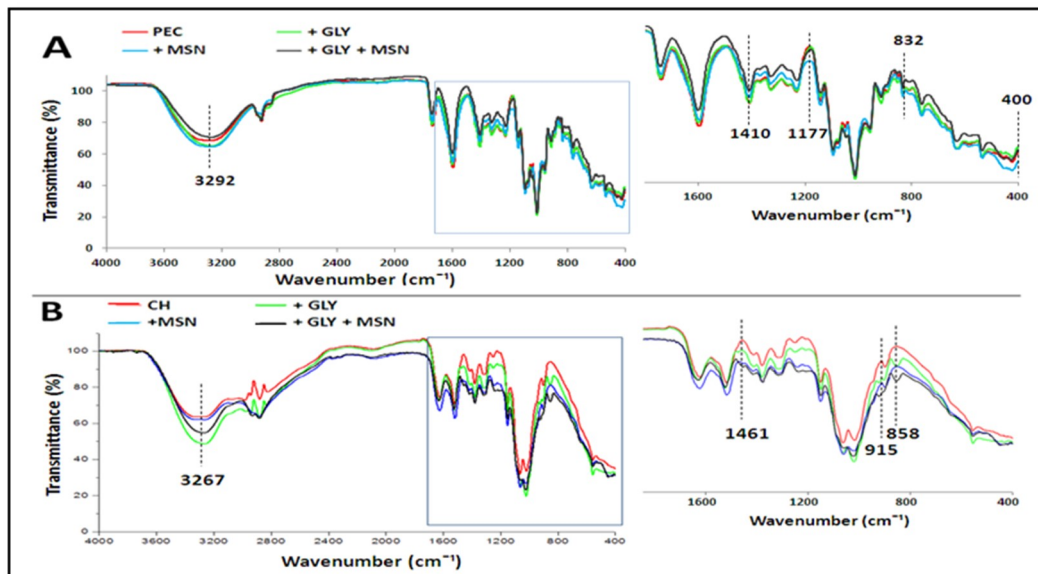


**Figure 2.** FT-IR spectra of PEC (A) and CH (B) films prepared in the presence or absence of GLY or MSN.

### 3.5. Film Moisture Content and Uptake

The prepared films were further characterized for their water moisture content and uptake, as these characteristics were extremely important for potential food packaging applications, especially, when water activity is high or when the film must be in contact with water, and acts as a food protective barrier [27]. In fact, higher moisture content might considerably limit edible film use as a packaging material. Figure 3 shows the positive influence of the MSNs on the film moisture content and uptake, indicating that the addition of MSNs to film-forming solutions significantly reduced both parameters, by using, both, PEC and CH as a film matrix, in the absence or presence of GLY, thus, suggesting that MSNs enhanced the moisture resistance of the prepared biomaterials. This phenomenon is likely due to the modified matrix structure by the hydrogen bond interaction between the two types of PSs and the nanoparticles. These results can be related to the interaction of nanoparticles, with both biopolymers, due to the hydrogen bonds, as described above. Consequently, the resulted dens network reduced the diffusion of water molecules into the matrix [28]. In fact, the equilibrium moisture uptake value depended on the film hydrophilic feature, as well as on its morphology. Therefore, MSNs probably produced a tortuous pathway and, consequently, a reduced water uptake. These findings were in agreement with the data previously reported for montmorillonite-containing films, made either with starch/carboxymethyl cellulose [29], or with methyl cellulose [30].

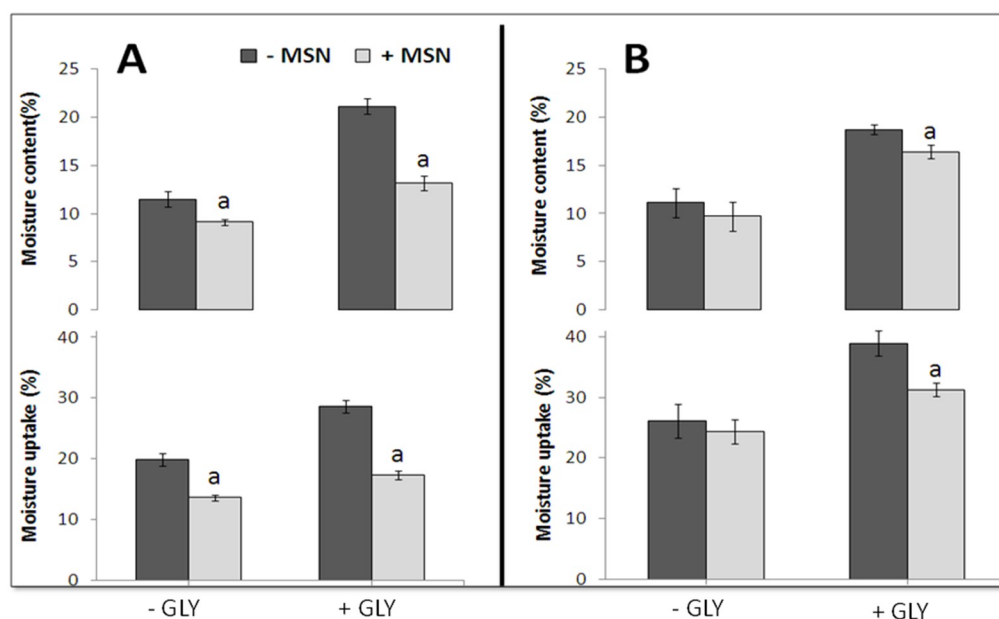


**Figure 3.** Effect of MSN on moisture-content and uptake of PEC (A) and CH (B) films, prepared with or without GLY. “a” values significantly different at  $p < 0.05$ , from those obtained without MSN.

#### 4. Conclusions

In the present study, PEC- and CH-based films, containing MSNs, were prepared by casting to obtain innovative biomaterials. FT-IR showed a strong interaction between PSs and nanoparticles, which influenced the behavior and the stability of both kinds of films. Morphology studies demonstrated an evident nanoparticle dispersion into the PEC matrix, as well as the absence of any nanoparticle agglomeration observed, conversely, in the CH-based films. MSNs were shown to decrease the moisture content and uptake of the prepared films, as a consequence of their interaction with both PEC and CH, by hydrogen bonds, and the formation of the resulting dens network which is able to reduce the diffusion of water molecules inside the biomaterial. In addition, MSN and GLY significantly increased the plasticity of both PEC- and CH-based biomaterials, also influencing their thickness and transparency. Therefore, MSNs are suggested as effective additives of PS-based films, for food industrial applications, when coatings or wrappings with reduced hydrophilic properties are required.

**Author Contributions:** Conceptualization, L.M. and R.P.; methodology, A.A., M.S., M.E., A.S. and M.C.; software, A.A., C.V.L.G., P.D.P.; validation, C.V.L.G., L.M. and R.P., formal analysis, L.M., and C.V.L.G.; investigation, A.A., M.E. and M.S.; resources, R.P, P.D.P.; data curation, L.M., P.D.P., A.S. and R.V.S.; writing—original draft preparation, C.V.L.G., R.P.; writing—review and editing, C.V.L.G., R.P., L.M.; visualization, A.A. M.E. and M.S.; supervision, L.M., P.D.P., R.P.; project administration, C.V.L.G.; funding acquisition, P.D.P. and R.P.

**Funding:** This work was supported by a grant to P.D.P., from the Italian Ministries of Foreign Affairs and International Cooperation (IV Programma Quadro di Cooperazione Italia/Messico, 2018-20, (CUP: E62D15002620001)) and R.P. was supported by the Agricultural, Food, and Forestry Policies (CUP: J57G17000190001). We are grateful to Mrs. Maria Fenderico for her helpful assistance.

**Conflicts of Interest:** The authors declare no conflict of interest.

#### References

- Rossi Marquez, G.; Di Piero, P.; Mariniello, L.; Esposito, M.; Giosafatto, C.V.L.; Porta, R. Fresh-cut fruit and vegetable coatings by transglutaminase-crosslinked whey protein/pectin edible films. *LWT Food Sci. Technol.* **2017**, *75*, 124–130. [[CrossRef](#)]
- Sabbah, M.; Porta, R. Plastic pollution and the challenge of bioplastics. *J. Appl. Biotechnol. Bioeng.* **2017**, *2*, 00033. [[CrossRef](#)]



3. Giosafatto, C.V.L.; Di Pierro, P.; Gunning, A.P.; Mackie, A.; Porta, R.; Mariniello, L. Trehalose-containing hydrocolloid edible films prepared in the presence of transglutaminase. *Biopolymers* **2014**, *101*, 931–937. [[CrossRef](#)] [[PubMed](#)]
4. Giosafatto, C.V.L.; Al-Asmar, A.; D'Angelo, A.; Roviello, V.; Esposito, M.; Mariniello, L. Preparation and characterization of bioplastics from grass pea flour cast in the presence of microbial transglutaminase. *Coatings* **2018**, *8*, 435. [[CrossRef](#)]
5. Krochta, J.M. Proteins as raw materials for films and coatings: Definitions, current status, and opportunities. In *Protein-Based Films and Coatings*, 1st ed.; Gennadios, A., Ed.; CRC Press: Boca Raton, FL, USA; New York, NY, USA, 2002; pp. 1–41.
6. Vodnar, D.C.; Pop, O.L.; Dulf, F.V.; Socaciu, C. Antimicrobial efficiency of edible films in food industry. *Notulae Botanicae Horti Agrobotanici Cluj-Napoca* **2015**, *43*, 302–312. [[CrossRef](#)]
7. Nascimento, T.A.; Calado, V.; Carvalho, C.W.P. Development and characterization of flexible film based on starch and passion fruit mesocarp flour with nanoparticles. *Food Res. Int.* **2012**, *49*, 588–595. [[CrossRef](#)]
8. Fernandez-Bats, I.; Di Pierro, P.; Villalonga-Santana, R.; Garcia-Almendarez, B.; Porta, R. Bioactive mesoporous silica nanocomposite films obtained from native and transglutaminase-crosslinked bitter vetch proteins. *Food Hydrocolloid* **2018**, *82*, 106–115. [[CrossRef](#)]
9. Mangiacapra, P.; Gorras, G.; Sorrentino, A.; Vittoria, V. Biodegradable nanocomposites obtained by ball milling of pectin and montmorillonites. *Carbohydr. Polym.* **2006**, *64*, 516–523. [[CrossRef](#)]
10. Mariniello, L.; Giosafatto, C.V.L.; Di Pierro, P.; Sorrentino, A.; Porta, R. Swelling, mechanical and barrier properties of albedo-based films prepared in the presence of phaseolin crosslinked or not by transglutaminase. *Biomacromolecules* **2010**, *11*, 2394–2398. [[CrossRef](#)] [[PubMed](#)]
11. Azuma, K.; Izumi, R.; Osaki, T.; Ifuku, S.; Morimoto, M.; Saimoto, H.; Minami, S.; Okamoto, Y. Chitin, chitosan, and its derivatives for wound healing: Old and new materials. *J. Funct. Biomater.* **2015**, *6*, 104–142. [[CrossRef](#)] [[PubMed](#)]
12. Sabbah, M.; Di Pierro, P.; Cammarota, M.; Dell'Olmo, E.; Arciello, A.; Porta, R. Development and properties of new chitosan-based films plasticized with spermidine and/or glycerol. *Food Hydrocolloid* **2019**, *87*, 245–252. [[CrossRef](#)]
13. Esposito, M.; Di Pierro, P.; Regalado-Gonzales, C.; Mariniello, L.; Giosafatto, C.V.L.; Porta, R. Polyamines as new cationic plasticizers for pectin-based edible films. *Carbohydr. Polym.* **2016**, *153*, 222–228. [[CrossRef](#)] [[PubMed](#)]
14. Tonyali, B.; Cikrikci, S.; Oztop, M.H. Physicochemical and microstructural characterization of gum tragacanth added whey protein based films. *Food Res. Int.* **2018**, *105*, 1–9. [[CrossRef](#)] [[PubMed](#)]
15. ASTM D882-97. *Standard Test Method for Tensile Properties of Thin Plastic Sheeting*; ASTM: Philadelphia, PA, USA, 1997.
16. Farhan, A.; Hani, N.M. Characterization of edible packaging films based on semi-refined kappa-carrageenan plasticized with glycerol and sorbitol. *Food Hydrocolloid* **2017**, *64*, 48–58. [[CrossRef](#)]
17. Singh, T.P.; Chatli, M.K.; Sahoo, J. Development of chitosan based edible films: Process optimization using response surface methodology. *J. Food Sci. Technol.* **2015**, *52*, 2530–2543. [[CrossRef](#)] [[PubMed](#)]
18. Manrich, A.; Moreira, F.K.V.; Otoni, C.G.; Lorevice, M.V.; Martins, M.A.; Mattoso, L.H.C. Hydrophobic edible films made up of tomato cutin and pectin. *Carbohydr. Polym.* **2017**, *164*, 83–91. [[CrossRef](#)] [[PubMed](#)]
19. Pacheco, N.; Naal-Ek, M.G.; Ayora-Talavera, T.; Shirai, K.; Román-Guerrero, A.; Fabela-Morón, M.F.; Cuevas-Bernardino, J.C. Effect of bio-chemical chitosan and gallic acid into rheology and physicochemical properties of ternary edible films. *Int. J. Biol. Macromol.* **2019**, *125*, 149–158. [[CrossRef](#)] [[PubMed](#)]
20. Liu, X.; Situ, A.; Kang, Y.; Villabroza, K.R.; Liao, Y.; Chang, C.H.; Donahue, T.; Nel, A.E.; Meng, H. Irinotecan delivery by lipid-coated mesoporous silica nanoparticles shows improved efficacy and safety over liposomes for pancreatic cancer. *ACS Nano* **2016**, *10*, 2702–2715. [[CrossRef](#)] [[PubMed](#)]
21. Shariatnia, Z.; Zahraee, Z. Controlled release of metformin from chitosan-based nanocomposite films containing mesoporous MCM-41 nanoparticles as novel drug delivery systems. *J. Colloid Interface Sci.* **2017**, *501*, 60–76. [[CrossRef](#)] [[PubMed](#)]
22. Rangelova, N.; Aleksandrov, L.; Nenkova, S. Synthesis and characterization of pectin/SiO<sub>2</sub> hybrid materials. *J. Sol-Gel Sci. Technol.* **2018**, *85*, 330–339. [[CrossRef](#)]

23. Nestic, R.A.; Kokunesoski, J.M.; Ilic, M.S.; Gordic, V.M.; Ostojic, B.S.; Micic, M.D.; Velickovic, J.S. Biocomposite membranes of highly methylated pectin and mesoporous silica SBA-15. *Compos. Part B*. **2014**, *64*, 162–167. [[CrossRef](#)]
24. Efimov, M.A.; Pogareva, G.V. IR absorption spectra of vitreous silica and silicate glasses: The nature of bands in the 1300 to 5000  $\text{cm}^{-1}$  region. *Chem. Geol.* **2006**, *229*, 198–217. [[CrossRef](#)]
25. Benmouhoub, N.; Simmonet, N.; Agoudjil, N.; Coradin, T. Aqueous sol-gel routes to bio-composite capsules and gels. *Green Chem.* **2008**, *10*, 957–964. [[CrossRef](#)]
26. Shariatinia, Z.; Fazli, M. Mechanical properties and antibacterial activities of novel nanobiocomposite films of chitosan and starch. *Food Hydrocolloid* **2015**, *46*, 112–124. [[CrossRef](#)]
27. Vejdani, A.; Mahdi Ojagh, S.; Adeli, A.; Abdollahi, M. Effect of  $\text{TiO}_2$  nanoparticles on the physico-mechanical and ultraviolet light barrier properties of fish gelatin/agar bilayer film. *LWT Food Sci. Technol.* **2016**, *71*, 88–95. [[CrossRef](#)]
28. Nasri-Nasrabadi, B.; Mehrasa, M.; Rafienia, M.; Bonakdar, S.; Behzad, T.; Gavanji, S. Porous starch/cellulose nanofibers composite prepared by salt leaching technique for tissue engineering. *Carbohydr. Polym.* **2014**, *108*, 232–238. [[CrossRef](#)] [[PubMed](#)]
29. Almasi, H.; Ghanbarzadeh, B.; Entezami, A.A. Physicochemical properties of starch–CMC–nanoclay biodegradable films. *Int. J. Biol. Macromol.* **2010**, *46*, 1–5. [[CrossRef](#)] [[PubMed](#)]
30. Tunç, S.; Duman, O. Preparation of active antimicrobial methyl cellulose/carvacrol/montmorillonite nanocomposite films and investigation of carvacrol release. *LWT Food Sci. Technol.* **2011**, *44*, 465–472. [[CrossRef](#)]



© 2019 by the authors. Licensee MDPI, Basel, Switzerland. This article is an open access article distributed under the terms and conditions of the Creative Commons Attribution (CC BY) license (<http://creativecommons.org/licenses/by/4.0/>).